Polar Bear (*Ursus maritimus*)

Supplementary material for *Ursus maritimus* Red List assessment

INTRODUCTION

Polar Bears (*Ursus maritimus*) are facing a range of threats that might impact their future population status (see section Threats below). The IUCN Polar Bear Specialist Group (PBSG) regards loss of sea-ice habitat due to climate warming as the most serious threat to future Polar Bear survival. We therefore based our Red List assessment on this threat factor only, recognizing that sea-ice conditions may not serve as a proxy for all environmental changes that could impact Polar Bears (e.g., changes in prey populations) and that secondary factors or potential threats could impact Polar Bears as well, particularly in the absence of management and mitigation (Amstrup *et al*. 2008, 2010; Atwood *et al*. 2015). A variety of methods exist to evaluate the effects of environmental change on population ecology (Sutherland 2006). For Polar Bears, several methods have been used evaluate the potential effects of sea-ice loss due to climate change, including structured elicitation of expert opinion through the Delphi method (O'Neill *et al*. 2008); Bayesian Networks to evaluate the potential effects of forecasted sea-ice extent and multiple qualitative stressors (e.g., Amstrup *et al*. 2007, 2008, 2010; Atwood *et al*. 2015); demographic projections or viability analysis using single-population models (e.g., Taylor *et al*. 2005, Lunn *et al*. 2014, Regehr *et al*. 2015); and mechanistic models describing vital rates as a function of environmental conditions or energetic factors for a single subpopulation (e.g., Molnar *et al*. 2010, Robbins *et al*. 2012b). To date, no analysis has used all available data on abundance for the 19 Polar Bear subpopulations (Figure 1; PBSG 2015) to evaluate the future status of the species as a function of estimated relationships between abundance and sea-ice conditions.

Here, we present a three-part analysis to explore the likelihood and magnitude of future population change for Polar Bears due to climate warming. This work was conducted for evaluating conservation status under the International Union for the Conservation of Nature (IUCN) Red List assessment using criterion A3c (IUCN 2014). First, we estimated generation length for Polar Bears using field data for all available subpopulations. Second, we derived a habitat metric by summarizing spatial and temporal characteristics of remote sensing data on sea-ice concentration, in a manner that was biologically relevant to Polar Bears. Third, we used statistical models and computer simulation to project the abundance of Polar Bear subpopulations forward in time over three Polar Bear generations, based on assumed and estimated relationships between abundance and habitat. Statistical models are commonly used in wildlife conservation to evaluate extinction risk, and in some situations can offer advantages over population models that require more parameters (Holmes et al. 2007). Our overall approach is framed as a sensitivity analysis, under which potential outcomes were explored for alternative relationships between Polar Bears and their habitats. These

relationships were established on the basis of expert opinion, published studies, and simplifications made to align the analytical approach with the sparse data available.

The goals of our analysis were: (1) to provide an updated numerical reference to the hypothesis that the carrying capacity of the Arctic marine environment supporting Polar Bears is proportional to the availability of sea ice; (2) to evaluate broad relationships between available data on Polar Bear abundance and derived sea-ice metrics representing Polar Bear habitat, including the ramifications of these relationships persisting into the future; and (3) to use findings from (1) and (2) to inform the current IUCN Red List conservation category for Polar Bears, while representing assumptions and uncertainties in a transparent manner.

We note that the response of Polar Bears to ecological change is likely to be variable in time and space (e.g., Bromaghin *et al*. 2015). Furthermore, Polar Bear subpopulations may be influenced by other ecological and anthropogenic factors, such as industrial development and human-caused removals (Atwood *et al*. 2015), which were not considered here. Considerable variability exists in current status and trends of Polar Bears across the circumpolar Arctic (PBSG 2014).

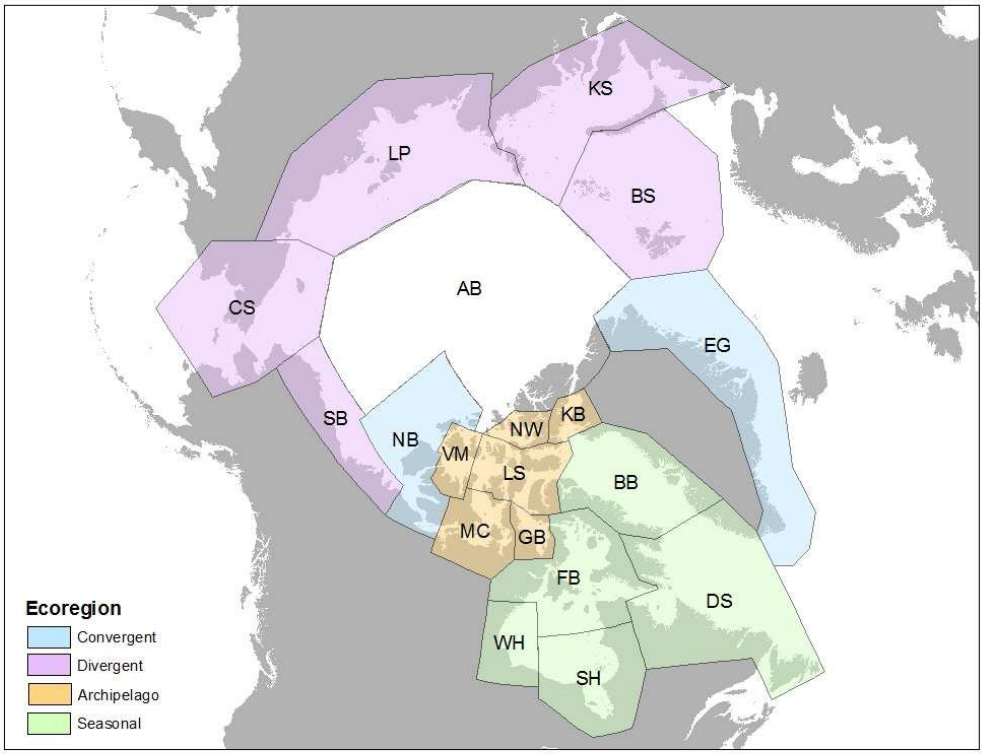

Figure 1. The 19 Polar Bear subpopulations (PBSG 2010) and the four Polar Bear ecoregions as proposed by Amstrup *et al.* (2007, 2008). The Polar Bear subpopulations are Arctic Basin (AB), Baffin Bay (BB), Barents Sea (BS), Chukchi Sea (CS), Davis Strait (DS), East Greenland (EG), Foxe Basin (FB), Gulf of Boothia (GB), Kane Basin (KB), Kara Sea (KS), Lancaster Sounds (LS), Laptev Sea (LP), M'Clintock Channel, (MC), Northern Beaufort Sea (NB), Norwegian Bay (NW), Southern Beaufort Sea (SB), Southern Hudson Bay (SH), Viscount Melville Sound (VM), and Western Hudson Bay (WH).

Of the 19 subpopulations, multiple lines of evidence suggest that two have experienced sea ice-related declines to date (Western Hudson Bay (WH), Stirling *et al*. 1999, Regehr *et al*. 2007, Lunn *et al*. 2014; and Southern Beaufort Sea (SB), Regehr *et al*. 2010, Bromaghin *et al*. 2015). Several subpopulations are either productive or stable despite sea-ice loss (Obbard *et al*. 2007, 2015; Stirling *et al*. 2011, Stapleton *et al*. 2012, Peacock *et al*. 2013, Rode *et al*. 2014), and several subpopulations are data deficient (PBSG 2015). Nonetheless, all Polar Bears depend on sea ice for fundamental aspects of their life history, and loss of sea ice is the primary long-term threat to the species (Amstrup *et al*. 2008, Laidre *et al*. 2008, USFWS 2008, Stirling and Derocher 2012). To represent this fundamental dependence we performed population projections using assumed and estimated linear relationships between habitat availability and Polar Bear abundance. Although the true functional form of relationships between habitat and abundance are likely to be complex (e.g., nonlinear), in light of the sparse data available we considered linear relationships useful for the purpose of exploring the directionality, magnitude, and uncertainty of potential population change.

METHODS

Generation Length

We used field data collected from 11 of 19 subpopulations of Polar Bears across the species' circumpolar range (Table 1) where physical captures provided information on age structure. Between 1967 and 2013, Polar Bears were captured on the sea ice in spring or the land in summer and fall. Bears one year and older were caught using chemical immobilization techniques (Schweinsburg *et al*. 1982, Stirling *et al*. 1989). Individual bears were identified by permanent tattoos applied to the inner surface of the upper lip. The reproductive status of an adult female (AF) was determined based on the presence of dependent young categorized as cub-of-the-year (C0), yearlings (C1), or two year-olds (C2). Age was determined by counting cementum annuli on a rudimentary premolar tooth extracted from bears >1 year old (Calvert and Ramsay 1998), and from body size and dentition for Polar Bears ≤1 year old. We used subpopulation boundaries per the International Union for the Conservation of Nature, Polar Bear Specialist Group (PBSG; PBSG 2010).

Generation length (GL) was calculated as the average age of parents of the current cohort (i.e., of newborn individuals in the population; IUCN 2012). We based GL on females only because Polar Bears are polygynous and genetic studies to determine paternity are rare. For each subpopulation, GL was calculated as the arithmetic mean of integer age for AFs with one or more C0, across all years for which field data were available. Approximate 95% confidence intervals for estimates of mean GL were determined using a bootstrap procedure with 1,000 replicates (Manly 1991). Adult females with one or more C1 in year t+1 were considered pseudo observations of AFs with C0 in year t. Maternity was not inferred based on observations of AFs with C2s, because some C2s were already weaned (and therefore no longer observable with their mother) by the months of March-May when most spring fieldwork occurred.

Multiple observations of an individual AF in year t were removed, as were instances of both a direct and pseudo observation (e.g., if the AF was captured in year t with a C0 and then in year t+1 with a C1). Multiple observations of an individual AF over different years, representing different reproductive events, were retained because excluding previously-captured AFs from the analysis would bias estimates of GL towards a pool of younger, previously un-captured mothers. If the survival of dependent young was

positively correlated with the mother's age, then inferring maternity based on observations of AFs with C1s could introduce positive bias into estimates of GL. We attempted to minimize potential bias based on relationships between maternal age and the survival or timing of weaning of dependent young, by not inferring maternity based on observations of AFs with C2s. We assumed aging errors from analysis of tooth cementum annuli were random, and thus field estimates of GL should not be biased by these errors, although standard errors could be underestimated. Possible biases include nonrandom aging errors as a function of bear age or subpopulation ecology (Christensen-Dalsgaard *et al*. 2010). Finally, sampling of AFs that were sighted during fieldwork was random with respect to age, and we assumed that the sightability of AFs was also independent of age.

Table 1. Estimates of mean generation length (GL) for 11 Polar Bear subpopulations where field data were available from capture programs. In some cases data were not available for all years within the specified period. The estimates reported in the effective sample size column may include one year prior to actual data due to creation of pseudo observations in year *t* based on observations of adult females (AF) with yearlings in year *t*+1. Effective sample size includes direct and pseudo observations, with a maximum of one observation per year per AF.

Subpopulation	Study Period	Effective sample size	Generation length (years)	95% CI lower	95% CI upper
Baffin Bay	1992: 1997 and 2009: 2013	170	11.6	11.0	12.4
Barents Sea	1992: 2013	298	11.8	11.3	12.4
Chukchi Sea	1990: 1994 and 2008: 2013	106	11.3	10.5	12.3
Davis Strait	2005: 2007	243	10.3	9.7	10.9
East Greenland	2007: 2008	5	9.6	6.8	12.4
Gulf of Boothia	1995: 2000	95	12.6	11.6	13.5
Lancaster Sound	1993: 1997	230	13.1	12.5	13.7
Northern Beaufort Sea	1972: 2006	172	11.4	10.7	12.2
Southern Beaufort Sea	1967: 2013	440	10.7	10.3	11.2
Southern Hudson Bay	1984: 2009	274	10.5	10.0	11.0
Western Hudson Bay	1968: 2013	1,341	13.7	13.4	14.0

Sea Ice

Polar Bears depend on sea ice as a platform for hunting. Sea ice also facilitates seasonal movements, mating, and in some areas maternal denning (see Summary Text for detail). Multiple approaches have been used to derive sea-ice metrics for use as predictors of Polar Bear body condition, reproduction, or survival. These metrics have generally reflected the number of reduced-ice days in summer (Obbard

et al. 2007, Peacock *et al.* 2013, Regehr *et al.* 2010, Rode *et al.* 2012, 2014) or the date of sea-ice breakup or formation (Cherry *et al.* 2013, Lunn *et al.* 2014, Stirling and Parkinson 2006, Regehr *et al.* 2007). The choice of metrics has been based on the ecology of Polar Bears within a specific region, and metrics of a similar type (e.g., based on reduced-ice days, but using different sea-ice concentration thresholds; Cherry *et al.* 2013, Rode *et al.* 2014) tend to be correlated.

We used expert opinion and findings from previous studies to develop a sea-ice metric that summarizes the annual availability of important habitats for Polar Bears. We used the *Sea Ice Concentrations from Nimbus-7 SMMR and DMSP SSM/I-SSMIS Passive Microwave Data* (Cavalieri *et al.*, 1996, updated yearly) available from the National Snow and Ice Data Center (NSIDC) in Boulder, CO, USA. This product is designed to provide a consistent time series of sea-ice concentrations (the proportion of ocean area covered by sea ice) spanning the coverage of several passive microwave instruments. The sea- ice concentrations are calculated using the NASA Team algorithm, and are provided on a polar stereographic grid (true at 70°N) with a nominal grid cell size of 25 × 25 km (the cell size varies slightly with latitude).

Spatial coverage of sea-ice concentration data includes the Arctic Ocean and sub-Arctic seas, except for a circular area approximately 1.2 × 106 km2 north of 84°N that was not covered by the early passive microwave satellites, referred to as the "pole hole" in satellite coverage (Figure 1). With the advent of a new satellite in 1987, the pole hole shrank but was not eliminated. The pole hole is entirely contained within the boundary of the Arctic Basin (AB) subpopulation and for our purposes were treated as if it were land, i.e. excluded from analysis. We define the pole hole according to its pre-1987 size and use that across all years for consistency of calculations.

Temporal coverage of sea-ice concentration data is every other day from 26 October 1978 through 9 July 1987, and then daily through 31 December 2014. We used linear interpolation to fill the alternating-day gaps prior to 9 July 1987, and to span a data gap from 3 December 1987 to 13 January 1988. For each day (1 January 1979 to 31 December 2014), we extracted the sea-ice concentrations within the boundaries of the 19 PBSG subpopulations (Figure 1). We then calculated the total sea-ice area by summing, over all grid cells with concentration greater than 15%, the product of sea-ice concentration and grid cell area. The result was a time series of daily sea-ice area within each subpopulation boundary.

We determined a sea-ice area threshold that is intended to mark the transition between summer and winter ice conditions. For each subpopulation, we calculated the mean September sea-ice area (denoted Area_Sept) and the mean March sea-ice area (denoted Area_March) over the period 1979-2014. The threshold area (denoted T) was chosen as the midpoint of these values:

$$T = \text{Area\_Sept} + (50\%) \times (\text{Area\_March} - \text{Area\_Sept})$$

The rationale is that sea-ice area reaches its annual minimum in September and its annual maximum in March, so the threshold should be a consistent point between the two. We then calculated the final sea-ice metric ice, which is the number of days per year (1979-2014) that sea-ice area exceeded the threshold T.

The metric *ice* represents our primary index for habitat quality and area of occupancy for Polar Bears. We calculated *ice* relative to the entire calendar year (i.e., a maximum possible value of 365 days) to avoid assumptions about periods when sea ice is most important to Polar Bears, even though sea-ice availability during the winter may be less important than during spring and autumn periods of increased foraging. Furthermore, we

calculated the metric ice using subpopulation-specific values of T, as opposed to using a fixed-area threshold for all subpopulations. This resulted in values of ice that were likely correlated with the availability of suitable habitat for a significant fraction of the Polar Bears within each subpopulation. We note that trends in *ice* were not sensitive to the choice of a sea-ice concentration threshold when summing sea-ice area over grid cells. Parkinson (2014) used the same sea-ice concentration products to calculate the number of ice-covered days per year, and found that trends over the period 1979-2013, and over shorter periods, were similar using 15% and 50% concentration thresholds to separate ice-covered from non-ice-covered grid cells.

For each subpopulation, we fit a simple linear regression with ice as the response variable and year (1979-2014) as the predictor variable ($\boldsymbol{ice} = B_0 + B_{year} \times \mathbf{year} + \varepsilon$; slope coefficients summarized in Table 2). Predicted values of *ice* for the year 2015 and for three Polar Bear generations into the future were used in subsequent calculations (see Population projections). Linear projections of the observed sea-ice metric are preferable to forecasts from global climate models for three reasons. First, there is considerable spread in projected sea-ice extent from global climate models through mid-century, both within and among different scenarios for greenhouse gas emissions (IPCC 2013), and there is no way to predict which emission scenario will play out. Instead of the many possible sea-ice realizations offered by the models, it is prudent to select the realization that the Arctic is actually experiencing, and project that realization into the future. Such a projection should be linear, as the sea-ice data do not support anything more complicated. Second, linear projections of observed sea-ice loss are generally more rapid than projections based on the ensemble mean of CMIP5 models through mid-century (Stroeve *et al*. 2012, Overland and Wang 2013). Therefore, our approach is precautionary for the purpose of conservation assessment, in the sense that it projects plausible but relatively rapid sea-ice loss compared to the alternative approach of using the CMIP5 ensemble mean. Third, linear projections of observed sea-ice loss can be derived for relatively small regions of the Arctic, whereas the spatial resolutions of most global climate models do not adequately resolve the channels and fjords of the Canadian Arctic Archipelago where several subpopulations of Polar Bears occur.

Table 2. Estimated slope, standard error (SE), and significance of least squared regressions fit to number of reduced-ice days (ice) for the 19 Polar Bear subpopulations over the period 1979-2014. Significance of the estimated slopes was determined by F- test: * 95% and ** 99%. The Polar Bear subpopulations and ecoregions are shown in Figure 1.

Subpopulation	Ecoregion	Slope (days/year)	SE	Significance
Arctic Basin	Convergent	-2.46	0.277	**
Baffin Bay	Seasonal	-1.27	0.216	**
Barents Sea	Divergent	-4.11	0.664	**
Chukchi Sea	Divergent	-0.90	0.213	**
Davis Strait	Seasonal	-1.71	0.367	**
East Greenland	Convergent	-1.07	0.308	**
Foxe Basin	Seasonal	-1.15	0.190	**
Gulf of Boothia	Archipelago	-1.88	0.368	**
Kane Basin	Archipelago	-1.44	0.416	**

Subpopulation	Ecoregion	Slope (days/year)	SE	Significance
Kara Sea	Divergent	-1.70	0.335	**
Lancaster Sound	Archipelago	-1.08	0.216	**
Laptev Sea	Divergent	-1.35	0.338	**
M'Clintock Channel	Archipelago	-1.12	0.274	**
Northern Beaufort Sea	Convergent	-0.93	0.328	*
Norwegian Bay	Archipelago	-0.73	0.263	**
Southern Beaufort Sea	Divergent	-1.75	0.363	**
Southern Hudson Bay	Seasonal	-0.68	0.239	**
Viscount Melville Sound	Archipelago	-1.26	0.391	**
Western Hudson Bay	Seasonal	-0.86	0.217	**

Population Projections

Abundance estimates

Estimates of subpopulation abundance were compiled from published and unpublished sources (Table 3). As there is no abundance estimate for the AB subpopulation, it was excluded from subsequent analyses. We approximated the variance of abundance estimates by assuming that the mean and 95% confidence intervals were based on a normal distribution. The mean coefficient of variation (CV) for estimates in Table 3 was 1.21. Estimates that did not include a quantitative assessment of uncertainty were assigned a CV of 0.50 for use in calculations. Estimates that were available as a range were assigned to the midpoint of the range. If a mean estimate of abundance was available over a multiyear period, it was assumed to be valid in the last year of the period.

Table 3 reflects a maximum of two abundance estimates per subpopulation, which served as the basis for one set of analyses as described subsequently. When multiple abundance estimates were available for a subpopulation, we selected two estimates on the basis of being broadly comparable (e.g., based on a similar geographic area) and separated by at least a decade, and thus representative of the mean numerical response of Polar Bears over a significant portion of the period 1979-2014 during which sea-ice data were available. Based on these criteria, 11 subpopulations had a single abundance estimate and seven subpopulations had two abundance estimates.

An additional set of analyses was performed that took advantage of time series of abundance estimates for relatively well-studied subpopulations. Time series were obtained from the published literature for the Southern Beaufort Sea (SB, 2002-2010; Bromaghin *et al.* 2015), Southern Hudson Bay (SH, 1985-1986, 2003-2005; Obbard *et al.* 2007), Northern Beaufort Sea (NB, 1979, 1985-1989, 2000, 2003-2006; Stirling *et al*. 2011), and Western Hudson Bay (WH, 1987-2011; Lunn *et al.* 2014) subpopulations.

Table 3. Abundance estimates for the 19 polar bear subpopulations. The Method column indicates capture-recapture study (CR), den count (DC), distance sampling (DS), expert opinion (EO), and other (O). NA indicates that estimates were not available.

Subpopulation	Abbreviation	Year	Estimate	95%_lwr	95%_uwr	Method	Reference
Arctic Basin	AB	NA	NA	NA	NA	NA	PBSG 2010
Baffin Bay	BB	1997	2,074	1,553	2,595	CR	Taylor *et al*. 2005
Barents Sea	BS	2004	2,644	1,899	3,592	DS	Aars *et al*. 2009
Chukchi Sea	CS	1997	2,000	NA	NA	EO	PBSG 2002
Davis Strait	DS	1996	1,400	NA	NA	EO	PBSG 1998
Davis Strait	DS	2007	2,158	1,833	2,542	CR	Peacock *et al*. 2013
East Greenland	EG	1997	2,000	NA	NA	EO	PBSG 2002
Foxe Basin	FB	1994	2,197	1,677	2,707	CR	Taylor *et al*. 2006
Foxe Basin	FB	2010	2,580	2,093	3,180	DS	Stapleton *et al*. 2012
Gulf of Boothia	GB	1986	900	NA	NA	EO	PBSG 1995
Gulf of Boothia	GB	2000	1,592	870	2,314	CR	Taylor *et al*. 2009
Kane Basin	KB	1997	164	94	234	CR	Taylor *et al*. 2008a
Kara Sea	KS	2013	3,200	NA[a]	NA	O	Matishov *et al*. 2014
Lancaster Sound	LS	1997	2,541	1,759	3,323	CR	Taylor *et al*. 2008b
Laptev Sea	LP	1993	1,000	NA	NA	DC/EO	Belikov and Randla 1987
M'Clintock Channel	MC	2000	284	166	402	CR	Taylor *et al*. 2006a
Northern Beaufort Sea	NB	1979	876	1[b]	1,844	CR	Stirling *et al*. 2011
Northern Beaufort Sea	NB	2006	1,004	1[b]	2,062	CR	Stirling *et al*. 2011
Norwegian Bay	NW	1997	203	115	291	CR	Taylor *et al*. 2008b
Southern Beaufort Sea	SB	1986	1,800	NA	NA	CR	Amstrup 1986
Southern Beaufort Sea	SB	2010	907	548	1,270	CR	Bromaghin *et al*. 2015
Southern Hudson Bay	SH	1986	1,000[c]	367	1,633	CR/EO	Kolenosky *et al*. 1992
Southern Hudson Bay	SH	2012	943	658	1,350	DS	Obbard *et al*. 2015

Subpopulation	Abbreviation	Year	Estimate	95%_lwr	95%_uwr	Method	Reference
Viscount Melville Sound	VM	1992	161	121	201	CR	Taylor *et al*. 2012
Western Hudson Bay	WH	1987	1,194	1,020	1,368	CR	Regehr *et al*. 2007
Western Hudson Bay	WH	2011	1,030	754	1,406	DS	Stapleton *et al*. 2014

[a] Estimates of uncertainty for the Kara Sea subpopulation were not used due to questions about the statistical methods in Matishov *et al.* (2013).

[b] Lower bound of the 95% CI set to 1, because it was negative based on the expected value and standard error provided in Stirling *et al.* (2011).

[c] Estimate of approximately 900 bears in Kolenosky *et al.* (1992) was revised to 1,000 by Canadian Polar Bear Technical Committee due to sampling issues (PBSG 2015).

Statistical models and computer simulation

We projected the abundance of Polar Bear subpopulations forward in time and evaluated percent change in mean global population size. Projections started in the year 2015 and ended in year t = 2015 + (3 × GL). To reflect uncertainty and variation in GL for Polar Bears, projections were performed using the mean, 5th percentile, and 95th percentile of subpopulation-specific estimates of mean GL (Table 1). Estimates of GL from field data may be shorter than natural GL due to human-caused removals. Therefore, use of the 95th percentile of GL reflected the potential for longer biological generation length (i.e., in the absence of human-caused removals) relative to estimates from field data. On average, the 95th percentile value of GL (13.6 years) was 1.9 years longer than the subpopulation-specific mean estimates. Based on expert opinion, 1.9 years is likely long enough to account for the effects of human-caused removals on GL, given that removal rates for most subpopulations were believed to be sustainable over the time period during which field data were collected. Although we considered three values of GL for the purpose of sensitivity analysis, inference regarding Red List conservation category was based on projections using the mean and 95th percentile of GL.

We used three analytical approaches to project Polar Bear subpopulations. Approach 1 assumed a one-to-one proportional relationship between the sea-ice metric (*ice*) and Polar Bear abundance (N) for each subpopulation. For example, a 10% decline in ice would equate to a 10% decline in N. Amstrup *et al*. (2007) projected carrying capacity for Polar Bears based on a similar relationship between density and habitat area. Also, a survey of 11 Polar Bear experts found that suspected percent change in total population size by the year 2050 was similar to suspected percent change in total habitat area (O'Neill *et al*. 2008).

Approaches 2 and 3 first estimated linear relationships between *ice* and empirical estimates of N, and then used these relationships to predict future abundance of each subpopulation as a function of predicted sea-ice conditions. Approach 2 estimated a global *ice*-N relationship (i.e., common to all subpopulations) using a reduced dataset that included a maximum of two abundance estimates for each subpopulation (Table 3). Under this approach, the seven subpopulations with at least two estimates of N exerted similar influence on the *ice*-N relationship. This represents the hypothesis that Polar Bears throughout their range exhibit broadly similar ecological and numerical responses

to changing sea-ice conditions. Approach 3 estimated ecoregion-specific ice-N relationships using an expanded dataset that included longer time series for the WH, SB, and NB subpopulations. Amstrup *et al*. (2007, 2008) proposed four Polar Bear ecoregions (Figure 1) based on variation in observed and forecasted sea-ice dynamics. Approach 3 represents the hypothesis that, within a specific ecoregion, the *ice*-N relationship estimated for subpopulations with available data (which included a single subpopulation within each of the Convergent, Divergent, and Archipelago ecoregions) applies to all other subpopulations within that ecoregion. Furthermore, Approach 3 assumed that the more numerous and precise annual abundance estimates for well- studied subpopulations represented a valid weight of evidence relative to the sparse data for less-studied or un-studied subpopulations. We expected results from Approaches 2 and 3 to be characterized by large uncertainty because of sparse data and large sampling error in abundance estimates for most subpopulations.

- Approach 1 estimated the proportional change in abundance for subpopulation i based on predicted values of mean *ice* for subpopulation i. For each subpopulation, we took the regression model for *ice* (as described above; slope coefficients summarized in Table 2) and simulated confidence intervals for the model coefficients using methods of Gelman and Hill (2006). Simulated confidence intervals did not include uncertainty in residual standard errors, and therefore represented uncertainty in predicted mean *ice* rather than the higher level of uncertainty in predicted individual realizations of *ice*. For each draw of the linear model coefficients, we predicted correlated values of mean *ice* for the years 2015 and t. We then derived an indicator for the proportional change in abundance of subpopulation i between years 2015 and t as: $\Delta N_{i,t} = (ice_{i,t} - ice_{i,2015}) / | ice_{i,2015} |$.

  Scaling subpopulation-specific changes to the global population requires consideration of the relative abundance of subpopulations. We used the most recent abundance estimate for each subpopulation (Table 3) as its starting abundance in year 2015 ($N_{i,2015}$). Uncertainty in $N_{i,2015}$ was simulated with 62,500 independent draws from a normal distribution with the estimated mean and standard error for each subpopulation. The lower bound of the distribution was set to 10% of the mean, to preclude implausibly-small starting values of abundance. For each draw of starting abundance for subpopulation i, we predicted mean abundance in year t as: $N_{i,t} = N_{i,2015} + \Delta N_{i,t} \times N_{i,2015}$. We then estimated mean global population size in 2015 (G_{2015}) and year t (G_t) by summing values of N_i over subpopulations. Finally, we calculated percent change in mean global population size as: $\Delta G = 100 \times (G_t - G_{2015}) / G_{2015}$.

- Approach 2 was similar to Approach 1, except that we included an additional step of estimating a relationship between ice and N, instead of assuming a one-to-one proportional change. Specifically, we used the reduced dataset to fit a linear model with normalized estimates of N (denoted Nnorm) as the response variable, and fitted values of ice (denoted fitted.ice, obtained from the subpopulation-specific regressions of ice vs. year) as the predictor variable. Normalization was performed separately for each subpopulation i, as follows: $N_i^{norm} = N_i / N_i^1$, where N_i is either the first or second available abundance estimate, and N_i^1 is

the first available abundance estimate. This scaled the first abundance estimate for each subpopulation to 1 and expressed the second estimate, if available, relative to 1. The effect was that changes in ice were related to proportional changes in subpopulation abundance, regardless of differences in the absolute abundance of the 19 subpopulations (e.g., under this approach, one less ice-covered day resulted in an X% change in subpopulation abundance, rather than a change of Y bears). For a given subpopulation, the two estimates of N were assumed to be independent on the basis of being separated by over a decade and, in some cases, resulting from different study methods (Table 3).

We used reciprocals of the variances of N^{norm} as weights in the fitting process, to account for differences in sampling uncertainty. Variances of N^{norm} were estimated from the variances of N using the delta method. The linear model for Approach 2 included an intercept for each subpopulation and a single, global slope coefficient ($N^{norm} = B_{BB} + B_{BS} + B_{CS} \ldots B_{WH} + B_{Global} \times \text{fitted.}\textit{ice} + \varepsilon$). Confidence intervals for model coefficients were simulated using 250 independent draws.

For each subpopulation we randomly selected 250 sets of predicted ice values for the years 2015 and t, from the 62,500 sets generated under Approach 1. For each set of *ice* values, we predicted correlated values of mean N for the years 2015 and t using the simulated model coefficients. We then estimated the proportional change in abundance of subpopulation i between years 2015 and t as: $\Delta N_{i,t} = (N_{i,t} - N_{i,2015}) / | N_{i,2015} |$. The 250 sets of *ice* values, each of which was used to predict 250 sets of N values, resulted in 62,500 point estimates of $\Delta N_{i,t}$ for each subpopulation. We then used estimates of $\Delta N_{i,t}$ to calculate percent change in mean global population size as described for Approach 1.

- Approach 3 differed from Approach 2 in two ways. First, calculations were applied to an expanded dataset created by merging the data in Table 3 with the time series of abundance estimates for relatively well-studied subpopulations (SB, SH, NB, and WH; section Abundance estimates). For each subpopulation, the expanded dataset included a maximum of one abundance estimate per year. We reduced year-to-year sampling variability in the longer time series for the SB and WH subpopulations with a three-point moving average, with weights ¼, ½, and ¼. The variances of averaged values were calculated from the standard formula for the variance of a sum, taking into account the covariances (e.g., Arnold 1990). Covariances were calculated from the lag-1 autocorrelation function of the time series, assuming a simple autoregressive (AR-1) model. Second, the linear model fit under Approach 3 included an intercept for each subpopulation and a slope for each ecoregion ($\mathbf{N}^{norm} = B_{BB} + B_{BS} + B_{CS} \ldots B_{WH} + B_{Seasonal} \times \textbf{fitted.}\textbf{\textit{ice}} + B_{Convergent} \times \textbf{fitted.}\textbf{\textit{ice}} + B_{Divergent} \times \textbf{fitted.}\textbf{\textit{ice}} + B_{Archipelago} \times \textbf{fitted.}\textbf{\textit{ice}} + \varepsilon$).

For all three approaches, indices of proportional change in subpopulation size ($\Delta N_{i,t}$) were constrained to the interval [-1, 1]. The lower limit of -1 reflects that abundance cannot be negative (i.e., cannot be reduced beyond 100% of its starting value). The upper limit of 1 reflects an assumption that the maximum potential abundance of each subpopulation is approximately two times current abundance. Conceptually, abundance could increase as a subpopulation approaches its carrying capacity or as carrying capacity itself increases (e.g., due to changing environmental conditions, such as thinner sea ice for high-latitude subpopulations). For each approach, results were summarized as the median and 95% confidence intervals of estimated percent change in mean

global population size (ΔG). We also estimated the probability of declines greater than 0%, 30%, 50%, and 80% based on the thresholds for threatened categories under criterion A3 of the IUCN Red List (Table 2.1, IUCN 2014).

Computations were performed using the R computing language (R Core Team 2015). The package "arm" was used to simulate confidence intervals for linear model coefficients (Gelman and Su 2015).

RESULTS

Generation length

Estimates of mean GL and 95% confidence intervals for 11 Polar Bear subpopulations are shown in Table 1. The median of subpopulation mean estimates was 11.4 years. The mean of subpopulation mean estimates was 11.5 years (95% CI = 9.8, 13.6). Mean estimates of GL for individual subpopulations ranged from 9.6 years (EG subpopulation; 95% CI 6.8-12.4) to 13.7 years (WH subpopulation; 95% 13.4-14.0).

Sea ice

The metric ice exhibited significant linear declines within all 19 Polar Bear subpopulation regions over the period 1979-2014 (Table 2). The mean decline across subpopulations was 1.45 days/year. The median decline was 1.26 days/year (95% CI = 0.71-3.37).

Population projections

We simulated percent change in mean global population size for nine scenarios, representing combinations of three values of GL and three assumptions for the relationships between ice and N (i.e., Approaches 1, 2, and 3; results in Table 4).

Approach 1 assumed a one-to-one proportional relationship between ice and N. For the year t = 2050 (i.e., using the global mean estimate of GL of 11.5 years) this approach suggested a median percent change in mean global population size of -30% (95% CI = -35%, -25%). The corresponding probability of a decline greater than 30% was approximately 0.56, and the probability of a decline greater than 50% was negligible.

Approach 2 estimated a global relationship between ice and normalized values of N using a maximum of two abundance estimates per subpopulation. The estimated slope coefficient was not significantly different from 0 and characterized by large uncertainty (Table 5). For the year t = 2050, Approach 2 suggested a median percent change in mean global population size of -4% (95% CI = -62%, 50%). The corresponding probability of a decline greater than 30% was approximately 0.20, and the probability of a decline greater than 50% was approximately 0.06.

Approach 3 estimated ecoregion-specific linear relationships between ice and normalized values of N that reflected the influence of additional abundance estimates for relatively well-studied subpopulations. Estimated slope coefficients were positive for the Seasonal and Divergent ecoregions (i.e., suggesting that decreasing ice was associated with decreasing N^{norm}), and negative but not statistically-significant for the Convergent and Archipelago ecoregions (Table 5). For the year t = 2050, Approach 3 suggested a median percent change in mean global population size of -43% (95% CI = -76%, -20%). The corresponding probability of a decline greater than 30% was approximately 0.86, and the probability of a decline greater than 50% was approximately 0.30.

Table 4. Simulation results for percent change in mean global population size.

Approach	Generation Length (years)	Percent change in mean global population size			Probability of decline		
		median	lwr 95% CI	upr 95% CI	x=0%	x=30%	x=50%
1	11.5	-30	-35	-25	1.00	0.56	0.00
1	9.8	-26	-31	-21	1.00	0.05	0.00
1	13.6	-34	-40	-29	1.00	0.95	0.00
2	11.5	-4	-62	50	0.55	0.20	0.06
2	9.8	-3	-55	44	0.55	0.16	0.04
2	13.6	-4	-68	56	0.55	0.24	0.08
3	11.5	-43	-76	-20	1.00	0.86	0.30
3	9.8	-41	-72	-19	1.00	0.84	0.25
3	13.6	-45	-79	-21	1.00	0.88	0.35

Table 5. Estimated slope, standard error (SE), and significance of linear models fit to abundance and sea-ice data. N^{norm} is normalized subpopulation abundance and ice is the sea-ice metric representing the number of ice-covered days per year. Significance of slope according to P-test: * 95% and ** 99%.

Approach	Region	Slope (N^{norm}/*ice*)	SE	Sig.	Number of abundance estimates per subpopulation used to estimate slope coefficient
2 2 SH, 2 WH	Global	<0.001	0.005		2 DS, 2 FB, 2 GB, 2 NB, 2 SB
3	Seasonal	0.013	0.002	**	2 DS, 2 FB, 6 SH, 24 WH
3	Convergent	-0.008	0.009		10 NB
3	Divergent	0.032	0.009	**	8 SB
3	Archipelago	-0.029	0.030		2 GB

DISCUSSION

We evaluated the potential response of the global Polar Bear population to alternative relationships between sea-ice conditions and subpopulation abundance. Our analyses included a comprehensive assessment of generation length for Polar Bears, development of a standardized sea-ice metric representing important habitat characteristics, and population projections using statistical models and computer simulation in conjunction with the best-available abundance data.

Approach 1 provides a numeric reference for population changes over three Polar Bear generations, based on the hypothesis of a one-to-one proportional relationship between sea-ice availability and Polar Bear abundance. Exclusion of the AB subpopulation, for which no estimate of abundance was available, was unlikely to have a significant effect on results from Approach 1. Although the AB region has experienced some of the most rapid sea-ice declines (Table 2), Polar Bear densities in this region are thought to be low and likely reflect seasonal or occasional use by bears with fidelity to adjacent subpopulations (PBSG 2010).

Accurate classification of extinction risk is difficult for short time-series of abundance estimates, particularly in the presence of sampling error and autocorrelated process variation (Connors *et al*. 2014). Furthermore, estimating population declines based on just two abundance estimates or using linear regression on a time series of abundance can be subject to false positives and false negatives (Wilson et al. 2011). Approaches 2 and 3 used abundance data for Polar Bears to fit simple statistical models with few parameters. Compared to more highly-parameterized population models, this method had the benefit of clearly propagating the effects of key assumptions (e.g., a linear relationship between *ice* and N^{norm}) on model outcomes. However, the method did not allow integration of data from multiple sources in a biologically-realistic population model (e.g., Rhodes *et al*. 2011), did not include mechanistic relationships between Polar Bear vital rates and environmental conditions (e.g., Regehr *et al*. 2015), and precluded consideration of non-linear behaviors or critical thresholds in population response (e.g., Derocher *et al*. 2013). Furthermore, our method did not consider the potential for spatial responses to sea-ice loss such as the alteration of subpopulation boundaries (Derocher *et al*. 2004).

Approaches 2 and 3 assumed that sea-ice dynamics have been the primary driver of observed changes in Polar Bear abundance (as mediated through changes in carrying capacity or intrinsic growth rate), that relationships between *ice* and N^{norm} were linear, and that estimated relationships will persist over three Polar Bear generations. By estimating a single, global relationship between *ice* and N^{norm}, Approach 2 did not reflect potential spatial patterns in the response of Polar Bears to ecological change (e.g., that lighter ice conditions could provide transient benefits to bears at higher latitudes, while limiting foraging opportunities at southerly latitudes). On the other hand, Approach 3 estimated ecoregion-specific relationships between *ice* and N^{norm} that were based on data for only a single subpopulation within each of the Convergent, Divergent, and Archipelago ecoregions. This did not reflect evidence for current variation in the response of Polar Bears to ecological change within several ecoregions (e.g., that the CS and SB subpopulations in the Divergent ecoregion appear to be responding differently to sea-ice loss; Bromaghin *et al*. 2015, Rode *et al*. 2014). Sparse data precluded a quantitative analysis of variation in population responses across ecoregions or other groupings.

Our findings appear consistent with expert-opinion assessments of the directionality and magnitude of future reductions in the global population of Polar Bears, although different methods and assumptions preclude direct comparison. Half of the participants in the survey by O'Neill *et al*. (2008) suspected at least a 30% decrease in global population size by 2050. Similarly, in the previous IUCN Red List assessment, Schliebe *et al*. (2008) suspected a population reduction of greater than 30% within three generations (45 years in that analysis) due to declines in area of occupancy, extent of occurrence, and habitat quality. In our analysis, across the six scenarios in Table 4 that projected abundance forward in time using the median and 95^{th} percentile of GL (i.e., excluding the 5^{th} percentile of GL, which is likely an underestimate of biological generation length), the

median percent change in mean global population size was approximately -32% (range -45% to -4%; Table 4).

Amstrup *et al*. (2007) used a deterministic model to relate carrying capacity for Polar Bears to forecasts of sea-ice availability from global climate models. Depending on the climate model used for sea-ice projections, that method suggested a 10%-22% reduction in global carrying capacity after 45 years, with the most pronounced declines in the Divergent and Seasonal ecoregions. Amstrup et al. (2007, 2008, 2010) and Atwood et al. (2015) used successive generations of a Bayesian Network to evaluate long-term threats to the persistence of Polar Bears. Atwood *et al*. (2105) suggested that Polar Bears could reach a dominant probability of a "greatly decreased" state (defined as occurring in reduced numbers or distribution that make Polar Bears difficult to detect and vulnerable to stressors) in the Divergent ecoregion by 2030, and perhaps as soon as 2055 in the Seasonal and Convergent ecoregions. Projections for the Archipelago ecoregion were less uniform, with a significant probability of remaining in a "same" or "decreased" state by the end of the 21st century. Qualitatively, the projected status of the four ecoregions would be ranked similarly based on the probability of decline in Atwood *et al*. (2015), or based on the sign and magnitude of ecoregion-specific slopes under Approach 3. However, different analytical frameworks and approaches to interpreting outcomes make comparison of our analysis with a Bayesian Network difficult. Furthermore, Atwood *et al*. (2015) considered a large suite of potential stressors for Polar Bears, and interactions among stressors, whereas our approach included only statistical (i.e., non-mechanistic) relationships between abundance and sea ice.

CONCLUSIONS

Our findings represent a sensitivity analysis based on limited data and several plausible but un-tested assumptions. When interpreted together and with the published literature, we suggest that the nine scenarios presented here provide a useful perspective on the potential response of Polar Bears to sea-ice loss, the primary long-term threat to the species. Approach 1 represents the assumption of a one-to-one proportional relationship between habitat availability and abundance. This simplifying assumption is commonly made in IUCN Red List assessments when population data are lacking (IUCN 2014). Approach 2 estimated a single relationship between *ice* and N^{norm} that was near 0 and not statistically significant. This reflects variability, uncertainty, and lack of evidence for changes in the mean global population size of Polar Bears over recent decades due to sea-ice loss (PBSG 2010). However, Approach 2 did not reflect that Polar Bears across their circumpolar range exhibit different patterns of feeding behavior, reproductive ecology, and space use. These differences, which likely reflect adaptations to local environmental conditions, can result in regional variability in the numerical response of Polar Bears to changing sea-ice conditions. In contrast to Approach 2, Approach 3 emphasized the potential effects of regional patterns in the numerical response of Polar Bears to sea-ice loss. In doing so, however, Approach 3 did not reflect variability in the status of subpopulations within ecoregions, and was heavily influenced by only a few relatively well-studied subpopulations, which may not represent the range of current and near-term responses. For example, the WH subpopulation contributed 24 data points to the analysis whereas the adjacent DS subpopulation contributed 2 data points (Table 5). Despite being in the same ecoregion, the WH and DS subpopulation regions encompass different habitats with respect to sea-ice extent and timing, continental shelf area, and seal species available to Polar Bears. Approach 3 also demonstrated the sensitivity of global projections to extrapolating inference from well-studied subpopulations to less-

studied subpopulations, which may be an oversimplification. For example, the ice-N relationship for the Divergent ecoregion, which contains approximately 1/3 of the total global population, was based solely on abundance estimates for a single declining subpopulation (SB).

Overall, our analysis highlights the potential for large reductions in Polar Bear abundance if sea-ice loss continues over the long-term, which is forecasted by climate models and other studies (IPCC 2013). It also highlights the large amount of uncertainty in even simple statistical projections of Polar Bear subpopulations, and the sensitivity of these projections to plausible alternative assumptions. Across the six scenarios in Table 4 that projected Polar Bear abundance forward in time using the median and 95th percentile of GL, the median probability of a reduction in the mean global population size greater than 30% was approximately 0.71 (range 0.20-0.95). The median probability of a reduction greater than 50% was approximately 0.07 (range 0-0.35), and the probability of a reduction greater than 80% was negligible. The IUCN Red List Guidelines suggest that assessors consider nearly the full range of uncertainty in potential outcomes, and adopt a precautionary but realistic attitude toward risk tolerance (Section 3.2.3, IUCN 2014). In light of the significant probability, across scenarios, of a reduction greater than 30%, and the relatively low probability of a reduction greater than 50%, we conclude that Polar Bears currently warrant listing as Vulnerable under criterion A3c (IUCN 2014).

References

For details of the references used, see the species account on The IUCN Red List web site.